International Journal of Applied Mathematics in Control Engineering 5 (2022) 136-144

Contents lists available at YXpublications

International Journal of Applied Mathematics in Control Engineering

Journal homepage: http://www.ijamce.com

Direct Torque Control with Linear State Observer for A Four-Phase SRM

Haonan Li, Huixian Liu, Linhou Yu, Ruohan Lu

School of Electrical Engineering, Hebei University of Science and Technology, Shijiazhuang 050018

ARTICLE INFO

Article history:
Received 5 September 2022
Accepted 20 December 2022
Available online 22 December 2022

Keywords:
Time-delay
Sliding mode control
Nonlinear system
Non-affine
Neural networks

ABSTRACT

A solution of direct torque control with a linear state observer for an 8/6 switched reluctance motor is proposed, aiming at the problem of large torque ripple. Firstly, the conventional current chopping control (CCC) scheme based on the mathematical model of the switched reluctance motor system is chosen in the controller design, and it has the disadvantage of large torque ripple, which has been proven by simulation. Secondly, the direct torque control (DTC) algorithm is developed to improve the torque ripple of the switched reluctance motor. And to further suppress the disturbance through the feed-forward link, a linear state observer (LSO) is also introduced to observe the load torque disturbance signal after the system is running stably. Finally, simulation results of the comparison between these methods verify the speed tracking performance and the influence of external disturbance on the 8/6 switched reluctance motor.

1. Introduction

Switched Reluctance Motor (SRM) has attracted more and more attention due to its simple structure, low cost, high reliability, and wide speed range. However, compared with traditional motors, a major disadvantage of SRM is that the torque ripple is relatively large, which limits its application.

The reason for the large torque ripple produced by SRM is mainly classified into the following aspects[1,2]: ①Double salient pole structure. ②Edge magnetic flux effect. ③Torque pulsation changes caused by power converter power supply. A new type of rotor tooth profile is proposed in [1], in which a semi-elliptical core is added on both sides of the rotor tooth. Despite the torque ripple can be reduced by changing the double convex structure, these methods increase the cost of motor manufacturing. An efficient direct method is to design the improving SRM stator and rotor poles, optimize the pole shoes and slot sizes of the stator and rotor poles, and improve the edge flux effect and magnetic circuit saturation of the motor [2]. Also, it is a reasonable way of optimizing the conduction mode to suppress rotation moment pulsation by connecting the full-bridge converter and SRM [3]. These three aspects introduced above are used to suppress the torque ripple of SRM from the main body and the control. Compared with the main body design, the control method has a lower cost.

Current Chopping Control (CCC) is a classic control of SRM. It usually adopts a fixed turn-on and turn-off angle and adjusts the phase current for control. But when the motor starts, the phase current rises rapidly, which may cause a large pulse current. More important, it may cause damage to the motor and power conversion devices, and the torque ripple of the motor is also large [4]. Direct Torque Control (DTC) attracts a large number of scholars with its advantages of simplicity, practicality, fast dynamic response, and high precision, and has done experiments to verify it. By analyzing the space flux vector and voltage vector of DTC for a four-phase switched reluctance motor, the switch on-off state has been established, and the torque ripple of the four-phase (8/6) SRM with DTC is reduced by 73% compared with the traditional torque control strategy [5]. In [6], new sector division method and control rules of DTC were proposed and carried out for the switched reluctance motor. The experimental results show that the improved DTC algorithm using 9-sector and 12-sector can indeed reduce torque ripple to a large extent. In [7], a three-phase 6/4 SRM based on space vector modulation direct torque control (DTC-SVM) was proposed. According to the expected changes of torque and flux, a suitable voltage vector with a certain amplitude and phase was calculated by fuzzy logic control. The aim of these control strategies is to realize the effective suppression of the torque ripple of the switched reluctance motor.

However, DTC still has the problem of not being able to accurately observe the influence of disturbance on the system in terms of torque ripple suppression. Therefore, a state observer is introduced on the basis of DTC in this paper. Observers are further subdivided into two classes: linear state observer (LSO for short)

* Corresponding author.
E-mail addresses: liuhuixian@hebust.edu.cn (H. Liu)
doi:

and nonlinear state observer [8]. An importance factor to take into account is the practicality. The linear state observer is designed as a feed-forward term to reduce the load disturbance. The LSO is mainly used to determine the internal state variables of the system through the observation of external variables. Through the control variable and output of the system, the measurable disturbance signals can be observed and compensated to controller. The innovation of this article is to establish a mathematical model of disturbance, and apply this model to obtain a LSO. The DTC-LSO based controller is proposed for a four-phase SRM system, the influence of the external disturbance on the system and the suppression and recovery under the disturbance are verified by simulation results

2. SRM Working Principle and Mathematical Model

2.1 SRM Structure and Operating Principle

SRM is a double salient pole variable reluctance motor, which is similar to reactive stepping motors. The salient poles of the stator and rotor are laminated by ordinary silicon steel sheets. The rotor has neither windings nor permanent magnets. There are concentrated windings on the stator poles. Two diametrically opposed windings are connected in series to form a two-pole magnetic pole. It is "one phase"[9]. This article introduces a four-phase (pole) SRM. The schematic diagram of the motor structure is shown in Fig. 1. Only the phase winding and its power supply circuit are drawn.

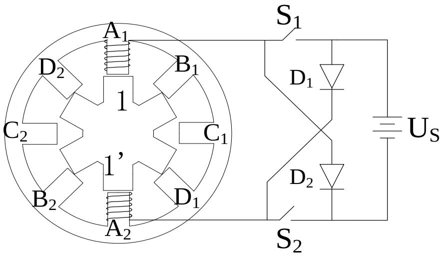

Fig. 1. Schematic diagram of the structure of a four-phase switched reluctance motor

The operating principle of SRM follows the principle of minimum reluctance, i.e., the magnetic flux always closes along the path of least reluctance [10]. In Fig. 1, when the stator A phase is excited, the generated magnetic force tries to make the rotor rotate to the position where the rotor 1-1' coincides with the stator pole axis A1-A2. At this position, the inductance of the A phase excitation winding is the largest and minimal resistance. The rotation direction of the SRM is always against the moving direction of the magnetic field axis. Changing the energization sequence of the motor stator winding can change the rotation direction of the motor, and changing the direction of the energized phase current does not affect the rotation of the rotor.

2.2 Numerical parameters

Under the circumstance that the core loss is ignored and the phase parameters and structure are symmetrical, the SRM system can be simplified and regarded as an electromechanical device with 4 pairs of electrical ports and a pair of mechanical ports, as shown in Fig. 2.

In Fig. 2, U_k is the stator phase winding voltage, where k=1, 2, 3, 4, and R_k is the stator phase winding resistance, i_k is the current of the stator phase winding, ψ_k is the stator phase winding voltage, J is the moment of inertia, T_e represents load torque, F is the viscous friction coefficient, and T_l is the load torque.

The dynamic process model of the electromechanical system shown in Fig. 2 is described as follows [11-12].

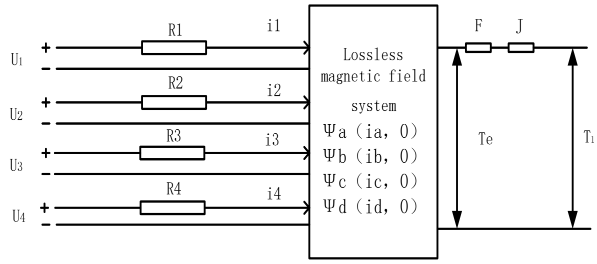

Fig. 2. Four-phase SRM system diagram

Voltage equation: according to the basic law of the circuit, the voltage applied to both ends of the windings of each phase of the stator is equal to the sum of the voltage drop of each phase of the stator and the induced electromotive force generated by the change of flux linkage. Therefore, the voltage balance equation of phase K of SRM can be written:

$$U_k = R_k i_k + \frac{d\Psi_k(\theta_k, i_k)}{dt} \tag{1}$$

In formula (1), U_k、i_k、R_k is the terminal voltage, current and resistance of the k-phase winding of the motor are successively, θ_k is the rotor position angle of phase K of the motor, $\Psi_k(\theta_k, i_k)$ is the flux linkage of phase K winding of the motor.

Flux linkage equation: the flux linkage of each phase winding of SRM is a function of phase current and self-inductance, other phase current and mutual inductance, and rotor position angle. Compared with self-inductance, the mutual inductance between SRM phases is small. In order to facilitate analysis, the phase-to-phase inductance can be ignored in the calculation of motor. Therefore, the flux linkage equation can be written as:

$$\Psi_k = L_k(\theta_k, i_k) i_k \tag{2}$$

In formula (2), $L_k(\theta_k, i_k)$ is the inductance of each phase, which is a function of phase current i_k and rotor position angle θ_k.

The following is the process of transforming equation (2) and deriving the partial differential of Ψ_k:

$$U_k = R_k i_k + \frac{\partial \Psi_k}{\partial i_k}\frac{di_k}{dt} + \frac{\partial \Psi_k}{\partial \theta}\frac{d\theta}{dt} \tag{3}$$

$$U_k = R_k i_k + \left(L_k + i_k \frac{\partial L_k}{\partial i_k}\right)\frac{di_k}{dt} + i_k \frac{\partial L_k}{\partial \theta}\omega \tag{4}$$

$$U_k = R_k i_k + e_t + e_m \tag{5}$$

In formula (5), $e_t$is the electromotive force induced by the change of flux linkage caused by current conversion, which is called transformer electromotive force. e_m is the electromotive force induced by the change of flux linkage in the winding caused by the change of rotor position, which is called moving electromotive force or motor electromotive force. e_m is directly related to the electromechanical energy conversion of SRM.

Mechanical motion equation: according to the mechanical principle, the mechanical motion equation of the rotor of SRM under electromagnetic torque T_e and load torque T_l can be written.

$$T_e = J\frac{d^2\theta}{dt^2} + K_\omega \frac{d\theta}{dt} + T_l \tag{6}$$

In formula (6), J is the moment of inertia of the system and K_ω is the friction coefficient. When the electromagnetic torque of the motor is inconsistent with the load torque acting on the motor shaft, the speed will change and produce angular acceleration.

It is expressed by $\frac{d\omega}{dt}$. Then $\omega = \frac{d\theta}{dt}$, the mechanical motion equation can be transformed into the following formula.

$$T_e = J\frac{d\omega}{dt} + K_\omega \omega + T_l \quad (7)$$

When the SRM operates stably, $\frac{d\omega}{dt} = 0$, then

$$T_e = K_\omega \omega + T_l = K_\omega \frac{d\theta}{dt} + T_l \quad (8)$$

According to the law of energy conservation, electromagnetic torque can be expressed as a function of magnetic common energy (output mechanical energy). Without considering the resistance loss, core loss and mechanical loss caused by rotor rotation, the electrical energy W_e input to the winding shall be equal to the sum of magnetic field energy storage W_m and magnetic common energy W_f.

The correlation equation of SRM describes the relationship between electromechanical energy conversion process and electromagnetic torque. The energy conversion of SRM meets the law of energy conservation. Take the current flux change curve of one phase of SRM winding to describe the energy conversion process, as shown in Figure 3.

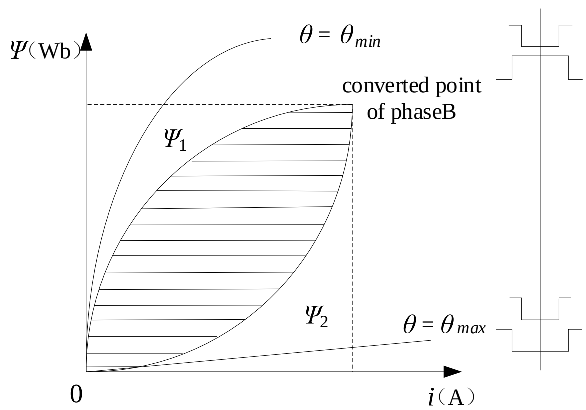

Fig. 3 curve of switched reluctance motor

The magnetization curves of the minimum and maximum reluctance positions correspond to $\theta = \theta_{min}$ and $\theta = \theta_{max}$ curves respectively. When the phase is on, the corresponding flux change curve is $\Psi_1 = \Psi_1(\theta, i)$. The current freewheeling in the relevant broken winding corresponds to $\Psi_2 = \Psi_2(\theta, i)$. In the process of motor rotation, the magnetic common energy W_f and magnetic energy storage W_m change nonlinearly. When one phase is on, it begins to rise along Ψ_1. When it reaches commutation point B, the winding flux reaches the maximum value. When the correlation is broken, the flux begins to fall along Ψ_2 and finally falls to zero.

Variation of magnetic common energy in the whole process:

$$\Delta W_f = \oint_\Omega \Psi di = \int_0^{ic} \Psi_2\, di - \int_0^{ic} \Psi_1\, di = \int \Psi_2 - \Psi_1\, di \quad (9)$$

Variation of magnetic energy storage:

$$\Delta W_m = \oint_\Omega i(\Psi, \theta) d\Psi = \int_0^{\Psi c} i_2\, d\Psi - \int_0^{\Psi c} i_1\, d\Psi = \int i_2 - i_1\, d \quad (10)$$

In formula (10), Ω represents the closed curve in Fig. 2; i_1 represents the inverse function $i_1 = i_1(\Psi, \theta)$ of flux linkage Ψ_1; i_2 represents the inverse function $i_2 = i_2(\Psi, \theta)$ of flux linkage Ψ_2.

From formula (9) and formula (10), it can be obtained that W_f and W_m are equal in size and are the shaded area, so:

$$\Delta W_f = -W_m \quad (11)$$

Since the change of magnetic common energy is the same as that of magnetic storage energy, and the change of magnetic common energy is the same as that of mechanical energy ΔW_a, it can be deduced that:

$$\Delta W_f = -W_m = \Delta W_a \quad (12)$$

According to the electromechanical energy conversion principle $\Delta W_a = T_{avg}\Delta\theta$,$T_{avg}$ is the average torque within the rotor rotation angle of $\Delta\theta$, so:

$$T_{avg} = \frac{\Delta W_f}{\Delta\theta} = -\frac{W_m}{\Delta\theta} = \frac{\Delta W_a}{\Delta\theta} \quad (13)$$

According to the method of taking limit in mathematics, it is deduced that the instantaneous torque at any point α on the closed curve is:

$$T_\alpha = \left.\frac{\partial W'}{\partial\theta}\right|_{i=const} = -\left.\frac{\partial W_f}{\partial\theta}\right|_{\Psi=const} \quad (14)$$

For formula (14), the instantaneous torque integral is averaged in one cycle to obtain the average torque. When evaluating the torque performance, the calculation of the average torque is very meaningful. The average output torque considering the symmetry of the motor winding is:

$$T = \frac{mN_r}{2\pi}\int_0^{\frac{2\pi}{N_r}} T_\alpha(\theta, i(\theta))\, d\theta$$
$$= \frac{mN_r}{2\pi}\int_0^{\frac{2\pi}{N_r}}\int_0^{i(\theta)} \frac{\partial W_m(\theta,\xi)}{\partial\theta} \xi d\xi d\theta \quad (15)$$

In formula (15), ξ is the intermediate variable of phase current, m is the number of phases of SRM, and N_r is the number of rotor teeth of SRM.

To sum up, the basic relations of switched reluctance motor are formula (5), formula (8) and formula (15). In theory, the established mathematical model of switched reluctance motor can accurately describe the electromechanical relationship of motor, but some variables are not easy to obtain, so there are different simplification methods in practical analysis.

3. SRM Control System Design

3.1 CCC Principle of SRM

Set the upper and lower limits of the phase current to i_{max} and i_{min} respectively, and the average value is i_{av} , the opening angle is θ_{on}, and the closing angle is θ_{off}, as shown in Fig. 4.

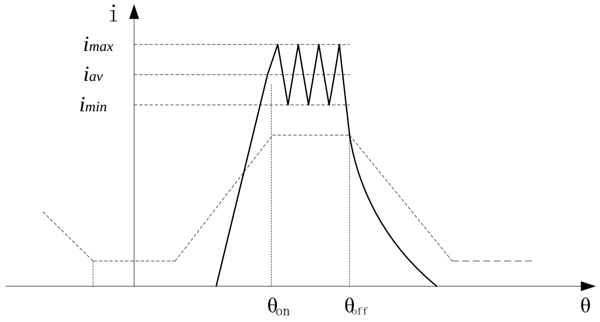

Fig. 4. Block diagram of CCC system

The actual current value obtained under current chopping control is i and the speed is ω. When the rotor position angle is between the opening angle and the closing angle and $i > i_{av}$, the switching device of the power converter is turned off. Otherwise it is turned on [13]. The control system block diagram is shown in Fig. 5.

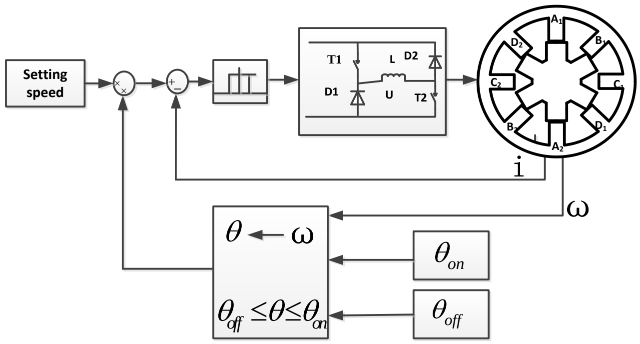

Fig. 5. Block diagram of CCC system

3.1 DTC Principle of SRM

Direct torque control is also known as direct self-control DSC in foreign original texts, which is directly translated as direct self-control. This idea of "direct self-control" takes torque as the center for comprehensive control. It is not only used to control torque, but also used for flux control and flux self-control. Direct torque control does not indirectly control torque by controlling current and flux linkage, but directly takes torque as controlled quantity. Its essence is to directly control stator flux linkage and electromagnetic torque by using space vector analysis method and stator magnetic field orientation [4]. This method does not need complex coordinate transformation, but directly calculates the mode and torque of flux linkage on the motor stator coordinates, and realizes PWM pulse width modulation and high dynamic performance of the system through direct tracking of flux linkage and torque. In fact, DTC selects the stator voltage vector according to the difference between the reference torque and stator flux vector and the actual value, and selects the stator voltage vector to limit and torque error within their respective flux and torque hysteresis bands.

For DTC, it is necessary to ensure that the vector size of the stator flux linkage does not change, and the torque is changed by increasing or decreasing $\Psi(k)$[14]. For Eq. (1), discrete form can be obtained after ignoring the influence of resistance,

$$\mathrm{U(k)} = \frac{\Psi(\mathrm{k})-\Psi(\mathrm{k}-1)}{\mathrm{dt}} \tag{16}$$

The deformation model,

$$\Psi(\mathrm{k}) = \Psi(\mathrm{k}-1) + \mathrm{U(k)T_s} \tag{17}$$

$\mathrm{T_s}$ is the sampling period.

The vector diagram is shown in Fig. 6.

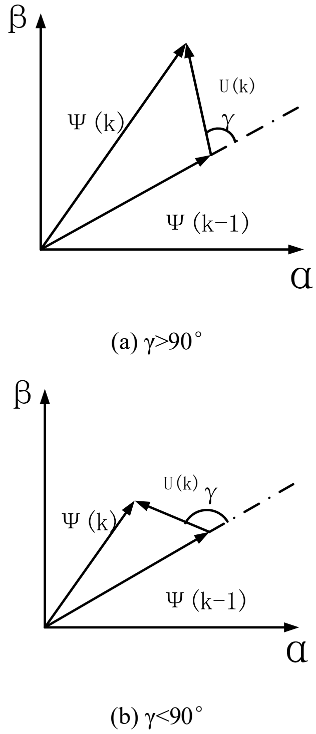

Fig. 6 . The relationship between stator flux vector and voltage vector

Definition the flux linkage of four-phase SRM,

$$\begin{cases}\Psi_\alpha = \Psi_a - \Psi_c \\ \Psi_\beta = \Psi_b - \Psi_d\end{cases} \tag{18}$$

$$\begin{cases}\Psi_s = \sqrt{\Psi_\alpha^2 - \Psi_\beta^2} \\ \delta = arc\tan\frac{\Psi_\beta}{\Psi_\alpha}\end{cases} \tag{19}$$

From Fig. 4, the relationship between the degree of γ and $\Psi(\mathrm{k})$ can be analyzed intuitively. In (a), when γ is greater than 90°, $\Psi(\mathrm{k})$ decreases. And when γ is equal to 90°, $\Psi(\mathrm{k})$ remains unchanged. In (b), when γ is less than 90°, $\Psi(\mathrm{k})$ increases. At this time, it is not difficult to find that since the stator flux linkage $\Psi(\mathrm{k}-1)$ is a fixed value, the magnitude of the voltage vector $\mathrm{U(k)}$ affects the magnitude of the stator flux linkage vector $\Psi(\mathrm{k})$, therefore, the choice of $\mathrm{U(k)}$ is very important.

The instantaneous torque can be obtained according to formula (14)

$$T_\alpha = \frac{\partial W'}{\partial\theta} = i\,\frac{\Psi(\theta,\mathrm{i})}{\partial\theta} \tag{20}$$

The Eq. (7) is transformed into the voltage equation about current rate of change:

$$\frac{di_k}{dt} = \frac{U_k - R_k i_k - \frac{\partial\Psi_k d\theta}{\partial\theta\ dt}}{\frac{\partial\Psi_k}{\partial i_k}} = \frac{U_k - R_k i_k - \frac{\partial\Psi_k}{\partial\theta}\omega}{L} \tag{21}$$

Eq. (16) is used to realize the increase or decrease of $\Psi(\mathrm{k})$. In a cycle, the current change is considered to be constant. Add or subtract the stator flux linkage can change the value of electromagnetic instantaneous torque. When $\frac{\partial\Psi(\theta,i_k)}{\partial\theta} > 0$ and $T_e > 0$, the stator flux is ahead of θ. When $\frac{\partial\Psi(\theta,i_k)}{\partial\theta} < 0$ and $T_e < 0$, the stator flux lags behind θ. Therefore, when the position angle θ of the stator flux linkage and the rotor is adjusted, the stator flux linkage can be changed, and then the torque is changed.

3.3 Voltage Vector of SRM

In this four-phase SRM motor system, the structure of the commonly used power converter adopts an improved asymmetric half-bridge. The working principle of this circuit and the asymmetric half-bridge are similar [15]. However, the improved circuit uses less two diodes and two switching devices, which reduces the cost. Moreover, the improved circuit can easily increase the number of winding phases, which is beneficial to reduce pulsation. The three vector states (1, 0, -1) of phase A are shown in Fig.7, and the current in these three states is unidirectional. The arrow in the figure is the direction of current flow. The "1" state indicates that the winding voltage is positive (the left is positive and the right is negative), the "0" state indicates that the winding voltage is zero, and the "-1" state indicates that the winding voltage is negative. The working principle of the "1" state is explained as follows. When the two switch tubes T_1 and T_2 connected to the winding are all turned on, the DC power supply forms a loop through T_1, L_A, and T_2, and the phase windings is bearing the positive voltage. The working principle of the "0" state is described as follows. Assuming that T_1 is off and T_2 is on at this time, since the inductance will hinder the change of current, L_A, T_2, and D_1 form a circulating current, which is a zero current loop. The working principle of the "-1" state is explained as follows. When T_1 and T_2 are all turned off, the DC power supply forms a loop through D_1, L_A, and D_2. At this time, the direction of the voltage applied to L_A is opposite to the "1" state. The phase winding voltage is reverse voltage.

Each voltage vector differs by 45° in turn, and the circle is divided into 8 regions with the angular bisector of every two voltage vectors as the boundary, and each region is set to N1 to N8, and each region is 45°. In the actual operation of the motor, when the four-phase winding at any time obtains a non-zero voltage, the corresponding state of the power switching device can only be selected from the above 8 types.

For a four-phase motor, the step angle is 15°, and the voltage vector is closely related to the flux linkage vector. When the input pulse is rotated by 15°, the flux linkage vector is rotated by an electrical angle of 90°. Under the stator coordinate system, eight space vectors of the four-phase SRM stator voltage are defined. They are named A (+) and C (-) coincide, B (+) and D (-) coincide, C (+) and A (-) coincide, D (+) and B (-) coincide. Take the four flux linkage vectors A (+), B (+), C (+), and D (+) as the basic vector, and then combine the basic vectors into 4 composite vectors, and the 8 flux linkage vectors are sequentially spaced with the phase difference is 45°, and the angular bisector of the eight voltage vectors (V1~V8) is used as the dividing line, then the voltage vector space is divided into eight vector spaces, as shown in Fig. 8.

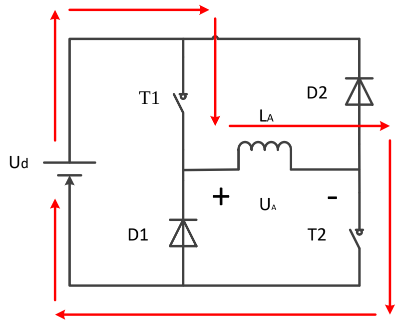

(a) Status 1

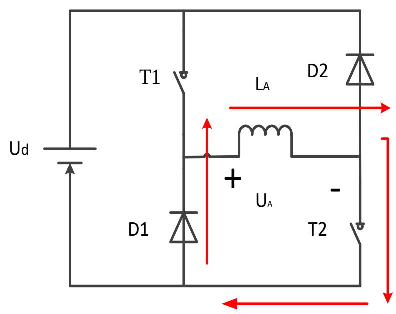

(b) Status 0

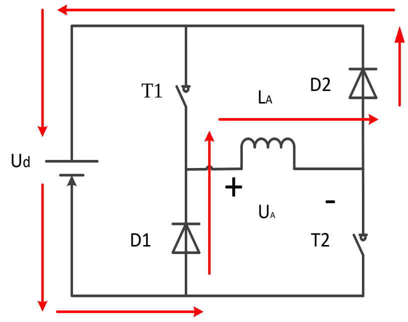

(c) Status -1

Fig. 7. Three level states of the power converter

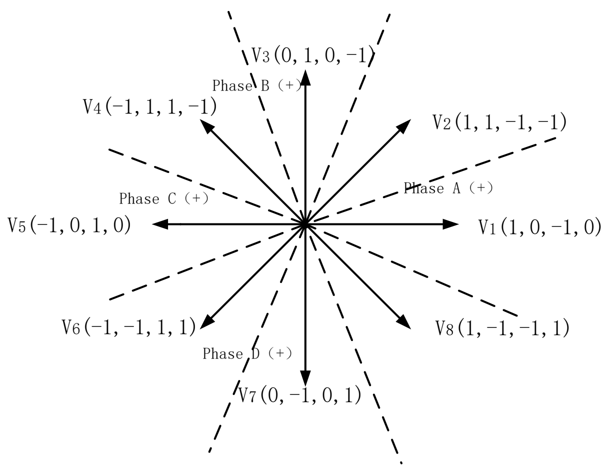

Fig. 8. Spatial voltage vector distribution diagram

Next the space voltage vector diagram is explained by taking V_2 as an example (A phase positive voltage, B phase positive voltage, C phase negative voltage, D phase negative voltage). V_2 (1, 1, -1,

-1) is synthesized from phase A and phase B, that is

$$\begin{aligned} V_2 &= V_a+V_b+V_c+V_d \\ &= 1\times V_a+1\times V_b-1\times V_c-1\times V_d \\ &= (1,1,-1,-1) \end{aligned} \tag{22}$$

where the maximum V_2 can be $2\sqrt{2}$.

For a four-phase SRM, its voltage vector has 81states. But not all of these 81 vector states are available. The illegal states include three phase of SRM simultaneous excitation, such as (1, 1, 1, 0), (1, 0, 1, 1), etc. All the SRM winding voltage are positive, negative or both 0 ((1,1,1,1) at the same time, i.e., (-1,-1,-1,-1), (0,0,0,0)). In addition, the two-step commutation principle should be followed to reduce the switching loss and the torque ripple of the device as much as possible. Hence, only one power device can be switched at a time. There is a detailed analysis of the principle of two-step commutation. During the control process, the conversion is carried out between the adjacent vectors. The switched order is in the form of +l↔0↔-1 (it can also be -l↔0↔+1, clockwise or anti clockwise). There is no direct conversion from +1 to -1. The loss generated is relatively small if the main switching device switches in the order of +l↔0↔-1. And because the voltage on the winding is reversed immediately during the process of +l↔-1, the winding is immediately demagnetized, so the resulting torque is relatively small. In the state change of l↔0, the winding flux is the same as before, which ensures that the phase torque will not be immediately weakened. As for the selection rule of the zero vector, it is necessary to ensure that it contains the "-1" state, which is beneficial to the demagnetization of the idle winding and ensures the correctness of the torque estimation. According to the above rules, the final switch table is shown in Table 1.

Table 1: The Corresponding Switch State of Each Voltage Vector

Voltage Space Vector	Switch Status	Voltage Space Vector	Switch Status
U1	(1，0，-1，0)	U5	(-1，0，1，0)
U2	(1，1，-1，-1)	U6	(-1，-1，1，1)
U3	(0，1，0，-1)	U7	(0，-1，0，1)
U4	(-1，1，1，-1)	U8	(1， -1，-1，1)

2.4 System Structure of DTC of SRM

According to the principle of SRM_DTC, the system structure diagram is constructed, as shown in Fig. 8.

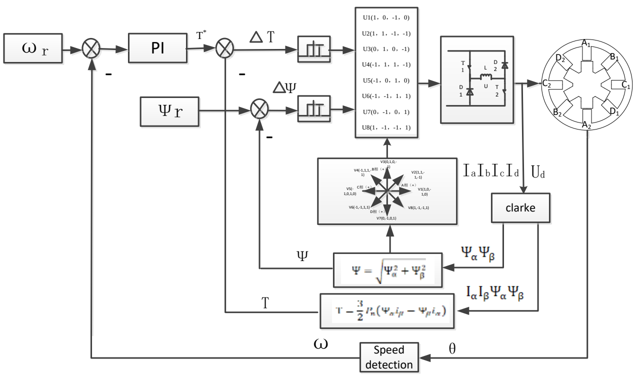

Fig. 9. SRM_DTC principal system structure diagram

It can be seen from Fig. 9 that this system is a double closed loop system, which consists of a speed loop and a magnetic link loop. The outer loop can regulate the speed response and the inner loop is used to maintain a constant magnetic link. The difference between the given speed and the feedback speed is set as the input of PI controller, then the torque T* can be obtained from the output. The torque T is calculated by the torque estimation according to the feedback winding current, voltage and position angle. After torque estimation，the flux linkage Ψ can be obtained from the feedback winding current, voltage and position angle. Finally, two differences, which is between T and T*, Ψ and the given flux linkage, are sent to the two hysteresis comparators, respectively.

2.5 Linear State Observer

LSO is introduced into the DTC system to observe the disturbance. The block diagram of the STC_LSO system is shown in Fig. 10[16-19].

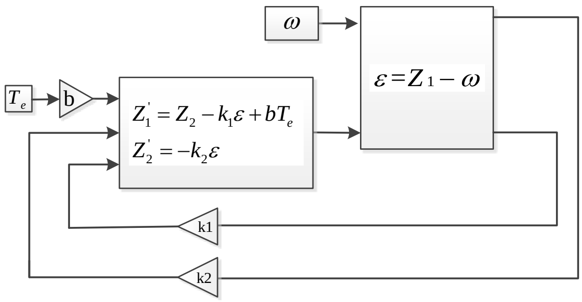

Fig. 10 . TC_LSO system block diagram

The equation of motion of SRM is shown in Eq. (3), and it can be modified as follows.

$$J\frac{d\omega}{dt} = T_e - T_l - F\omega \tag{23}$$

where J is the moment of inertia, T_e is the electromagnetic torque, T_L is the load torque, and F is the damping coefficient.

Then,

$$\frac{d\omega}{dt} = -\frac{T_l}{J} - \frac{F}{J}\omega + \frac{T_e}{J} \tag{24}$$

Let $a(t) = -\frac{T_l}{J} - \frac{F}{J}\omega, b = \frac{1}{J}$, Eq.(12) can be changed as follows.

$$\frac{d\omega}{dt} = a(t) + bT_e \tag{25}$$

The basic principle of the linear state observer is shown in Eq.

$$\begin{cases} \varepsilon = Z_1 - \omega_r \\ Z_1' = Z_2 - k_1\varepsilon + bu(t) \\ Z_2' = -k_2\varepsilon \end{cases} \tag{26}$$

where, ε is the error ,ω_r is the given speed, Z_1 is the speed feedback, Z_2 is the disturbance observation, k_1、k_2 is the feedback gain, $k_1 = 2\omega_1$, $k_2 = \omega_1^2$. There the ω_1 is the bandwidth of the expanded state observer, $\omega_1 = 3{\sim}5\omega_2$.

4. Simulation verification of SRM in multi control mode

Based on MATLAB / Simulink platform, the simulation diagram of direct torque control of four phase switched reluctance motor is built, as shown in Figure 11.

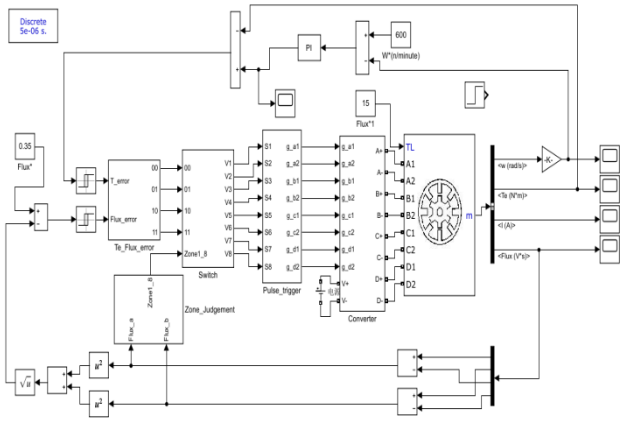

Fig. 11. Simulation model of four phase SRM direct torque control

The simulation parameters are set as follows: power supply voltage 220V, maximum flux linkage 1.1 Wb, maximum current is 88A, reference flux linkage is 0.35 Wb. The torque and flux linkage hysteresis width are set to ±0.1 and ±0.01, respectively. DC power supply 72V, reference speed$\omega_r = 600rpm$, stator resistance$\mathrm{R_s} = 0.014\Omega$, moment of inertia $\mathrm{J} = 0.0013\mathrm{kg \cdot m \cdot m}$, damping coefficient$\mathrm{F} = 0.02\mathrm{N \cdot m \cdot s}$, reset maximum torque $\mathrm{T_{max}} = 12\mathrm{N \cdot m}$.

The simulation results are shown in Figure 12. It can be seen from the simulation results that the speed rises rapidly, is consistent with the set speed at 0.06s, and maintains stable operation. During starting and operation, it shows the advantages of smooth and stable speed and small torque ripple.

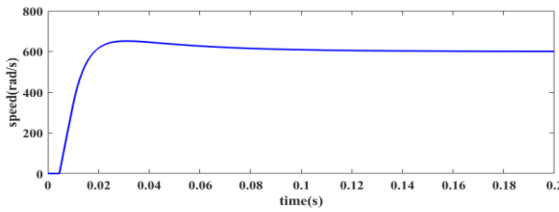

(a) Startup process and steady-state operating speed

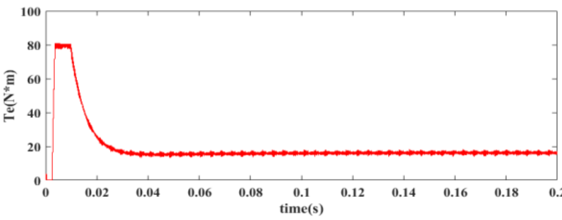

(b) Starting process and steady-state operating torque

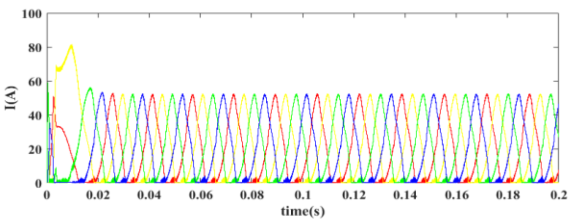

(c) Starting process and steady-state operating current

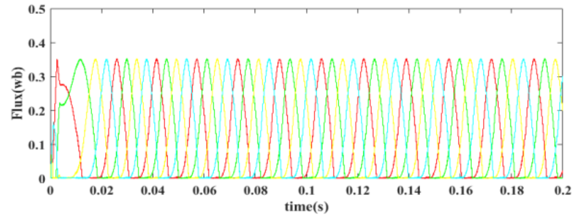

(d) Starting process and steady-state operation flux linkage

Figure 12 Simulation results of four phase SRM direct torque control

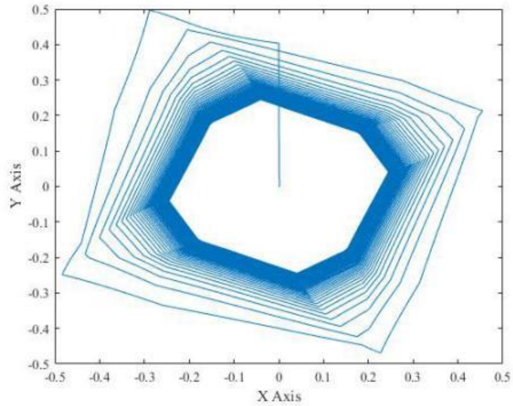

(a) CCC stator flux trajectory

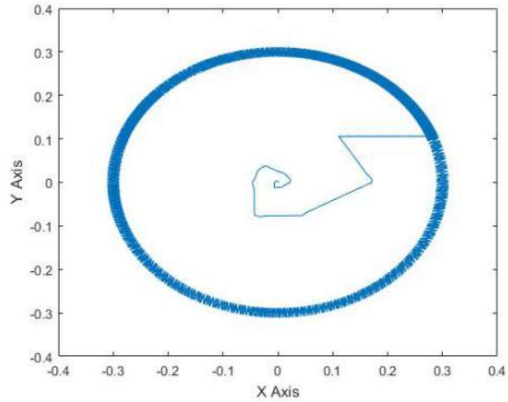

(b) DTC stator flux trajectory

Fig. 13. Stator flux trajectory

Torque waveform comparison is shown in Fig. 14. It can be seen that the torque fluctuation range is about 50~140 N.m under the CCC after the operation is stable, while it is about 10 ~ 13 N.m under the DTC. And the fluctuation range is only about 3N.m, the torque ripple of SRD is greatly reduced.

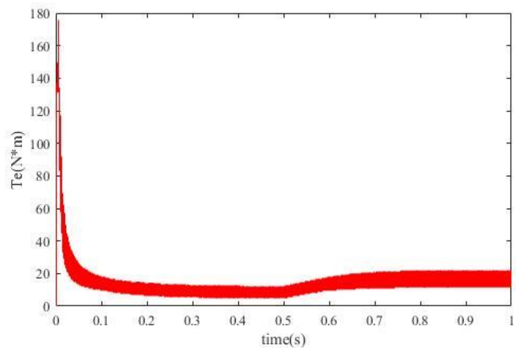

(a) CCC

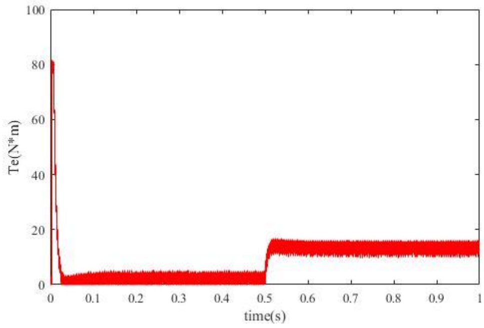

(b) DTC

Fig. 14. Torque responses under CCC and DTC

By comparing the stator flux trajectory in the two control modes (shown in Fig. 13), it can be seen that the stator flux trajectory under DTC is an approximate circular magnetic flux linkage, which is more accurate than CCC. The trajectory can control the motor more effectively, indicating that DTC has a better control result.

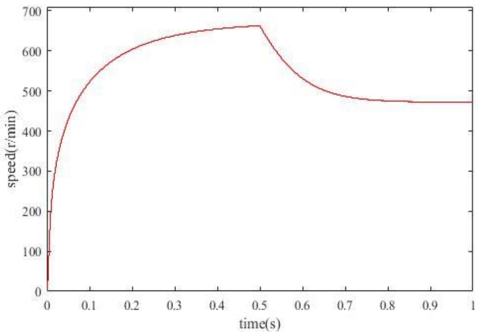

(a) CCC

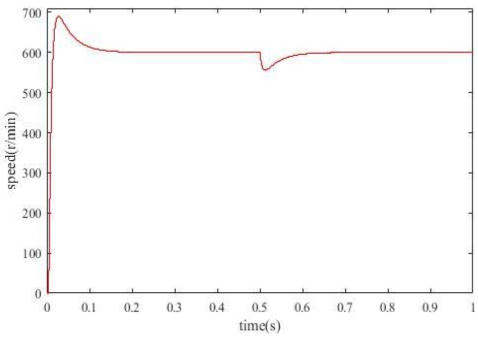

(b) DTC

Fig. 15. Speed responses under CCC and DTC

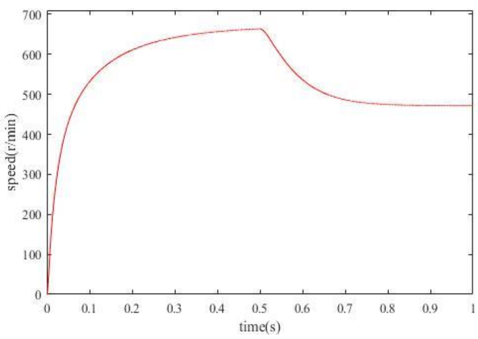

(a) CCC+LSO

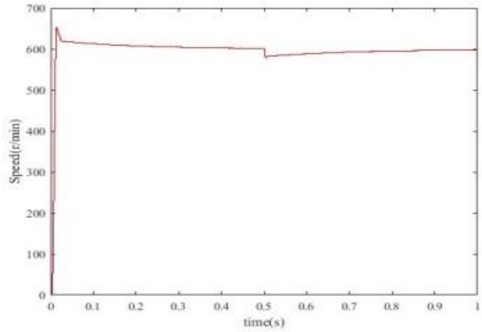

(b) DTC+LSO

Fig. 16 . Speed observer under CCC+LSO and DTC+LSO

Fig. 15 and 16 show that DTC reaches the set speed at 0.1 and runs smoothly (disturbance is added at 0.5s), while CCC can reach stability in about 0.8s, and the speed cannot reach the initial stable speed after being disturbed. The LSO is added to the two control systems, respectively. The results show that the LSO can accurately track the speed and observe the disturbance, and gets a good improvement for the torque ripple of SRM.

5. Conclusions

This article starts with the causes of torque ripple. Then the control principles of CCC and DTC are developed with the mathematical model of a four-phase 8/6 SRM. A LSO is also introduced to the control schemes to reduce the effect of disturbance and torque ripple. The simulation results demonstrate that DTC has a certain suppression effect on torque ripple. The LSO can accurately observe the measured disturbances on the system and compensate them as a feed-forward term. Next, the research on torque ripple suppression will be carried out on the combination of the ontology and the control methods.

References

Jing Libing, Cheng Jia. Torque ripple optimization for a switched reluctance motor [J]. Journal of Vibration and Shock, 2019 ,38(21):120-125.

Li Zhe, Zheng Ling, et al. Research on torque ripple and structure optimization of switched reluctance motor [J]. Electric Machines and Control, 2018,22(06):11-21

Nan Jiang, Fang Qi. Research on Performance of Two Different Structure Switched Reluctance Motors [J]. International Journal of Applied Mathematics in Control Engineering 3 (2020) 121-127

Yan Ning, Cao Xin, et al. Direct Torque Control of Switched Reluctance Motors Based on Full-bridge Converter [J].Proceedings of the CSEE. 2018,38(S1):235-242.

Tian Dexiang, Qu Bingni, et al. An Analytical Method of PWM Duty Cycle for Switched Reluctance Motors Based on Current Chopping Control [J]. Transactions of China Electrotechnical Society. 2019, 4(21): 4449-4457.

YANG Z，SHANG F, BROWN I P, at el. Comparative study of interior permanent magnet, induction, and switched reluctance motor drives for EV and HEV applications [J]. IEEE Transactions on Transportation Electrification, 2015, 1(03): 245-254.

D. Cheng, R. Ortega, E. Panteley, On port controlled Hamiltonian systems. Advanced Robust and Adaptive Control –Theory and Applications, D. Cheng, Y. Sun, T. Shen, H. Ohmori, Eds. Beijing: Tsinghua University Press, 2005: 3-16.

SOZER Y, HUSAIN I, TORRY D A. Guidance in selecting advanced control techniques for switched reluctance machine drives in emerging applications [J]. IEEE Transactions on Industry Applications, 2015, 51(06) 4505-4514.

Gao Qinhe,Dong Jiachen. Discussion on observation error of linear extended state observer [J]. Control and Decision , 2019, 34 (12): 2576-2584.

Wang Mianhua. Comparing Research of Multiple Control Strategies Simulating for SRM [J]. Journal of System Simulation, 2007 (20) :4844-4847.

Zhou Kai, Shi Zeng, Torque ripple reduction technique for switched reluctance motor [J]. Electric Machines and Control, 2019,23 (12):85-92.

Qing Long, Wang Huimin, et al. A High Efficiency Torque Ripple Suppression Method for Switched Reluctance Motor [J]. Transactions of China Electrotechnical Society. 2020,35 (09) : 1912-1920.

Ma Mingyao, et al. Subsection PWM Variable Duty Cycle Control of Switched Reluctance Motor Based on Current Soft Chopping [J]. Proceedings of the CSEE. 2018,38(18):5582-5589.

Zhang Xiaoping, et al. Research on Control Strategy of Switched Reluctance Motor Drive System for Mine Electric Locomotive [J]. Journal of System Simulation, 2016,28(11):2771-2776+ 2783.

A. Xu, C. Shang, J. Chen, J. Zhu and L. Han, "A New Control Method Based on DTC and MPC to Reduce Torque Ripple in SRM," in IEEE Access, vol. 7, pp. 68584-68593, 2019

Han Jingqing, From PID Technique to Active Disturbances Rejection Control Technique [J]. Control Engineering of China,2002 (03):13-18.

Han Jingqing, Auto Disturbances Rejection Control Technique [J]. Frontier Science,2007(01):24-31.

Yu Wentao, et al. Speed Control of Switched Reluctance Motor Using Polynomial Interpolation Speedometer and LADRC[J]. Electric Machines & Control Application 2020,47(12):17-24 + 48

Liu Zhiyong, et al. Method on aerial reluctance switched speed-torque control based on auto-disturbances rejection [J]. Electric Machines and Control,2020,24(04):113-120.2

Li Haonan was born in Shijiazhuang, China, in 1995. At present, he is studying for a master's degree in the school of electrical engineering of Hebei University of science and technology. In 2017, he obtained an engineering degree from the College of science and technology of Hebei University of science and technology. His main research field is the control and fault analysis of switched reluctance motor.

Liu Huixian was born in Ningjin, China, in 1984. She received the PhD. degree in control theory and control engineering from Southeast University, Nanjing, China, in 2012.

Since 2011, she has been with the School of Electrical Engineering, Hebei University of Science and Technology, where she is currently an Associate Professor.

Her research interests include nonlinear system control, predictive control with applications to AC motors.

Yu Linhou is currently studying for a master's degree in the School of Electrical Engineering, Hebei University of Science and Technology, Shijiazhuang, China. He received a bachelor's degree from Hebei University of Science and Technology in 2019. His main research area is the control of switched reluctance motors.

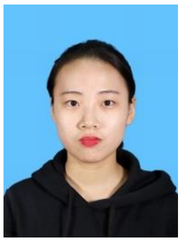

Lu Ruohan is currently studying for a master's degree in the School of Electrical Engineering at Hebei University of Science and Technology. She received her bachelor's degree from Zhengzhou Institute of Business and Technology in 2017. Her research interest covers motor control, sliding mode control and control applications.